

RESEARCH ARTICLE

Preparation and characterization of TiO₂/Pebax/(PSf-PES) thin film nanocomposite membrane for humic acid removal from water

Naeema Cheshomi¹  | Majid Pakizeh¹ | Mahdiah Namvar-Mahboub²

¹Department of Chemical Engineering, Faculty of Engineering, Ferdowsi University of Mashhad, Mashhad 91779-48974, Iran

²Department of Chemical Engineering, University of Gonabad, Gonabad, Iran

Correspondence

Majid Pakizeh, Department of Chemical Engineering, Faculty of Engineering, Ferdowsi University of Mashhad, Mashhad, Iran.
Email: pakizeh@um.ac.ir

New thin film composite (TFC) membrane was prepared via coating of Pebax on PSf-PES blend membrane as support, and its application in wastewater treatment was investigated. To modify this membrane, hydrophilic TiO₂ nanoparticles were coated on its surface at different loadings via dip coating technique. The as-prepared membrane was characterized using Fourier transform infrared spectroscopy, scanning electron microscopy (SEM), field emission SEM, and contact angle analysis. The Fourier transform infrared spectroscopy analysis and surface SEM images indicated that TiO₂ was successfully coated on the membrane surface. In addition, the results stated that the hydrophilicity and roughness of membrane surface increased by addition of TiO₂ nanoparticles. Performance of TFC and modified TFC membranes was evaluated through humic acid removal from aqueous solution. Maximum permeate flux and humic acid rejection were obtained at 0.03 and 0.01 wt% TiO₂ loadings, respectively. Rejection was enhanced from 96.38% to 98.92% by the increase of feed concentration from 10 to 30 ppm. Additionally, membrane antifouling parameters at different pressures and feed concentration were determined. The results indicated that surface modification of membranes could be an effective method for improvement of membrane antifouling property.

KEYWORDS

humic acid, Pebax, surface modification, thin film composite membrane, TiO₂ nanoparticles

1 | INTRODUCTION

Natural organic materials (NOMs) constitute an important group of surface water contaminants, which primarily consists of humic substances.^{1,2} Additionally, the NOMs may react with chlorine compounds during chlorination process of water, which lead to formation of some carcinogenic disinfectant by-products such as trihalomethanes and haloacetic acids.³ Thus, it is required to eliminate NOMs or its by-products from wastewater to have a healthy environment. According to their solubility in different pH, NOMs can be categorized into 3 groups: humic acid (HA), fulvic acid, and humin.^{4,5} Since HA is an important part of NOMs, it has been used as a sample model of these compounds in many researches.⁶

Up to now, different separation processes have been developed to remove HA from water, including adsorption,^{7,8} advanced oxidation processes,^{9,10} coagulation,^{11,12} and ultrafiltration (UF) process.¹³⁻¹⁶ Among these techniques, UF has attracted the researcher's attention

due to its low costs, low energy consumption, no need of change in phase, and compatibility with the environment.^{17,18}

Ultrafiltration membranes have been prepared in both "asymmetric" and "composite" structures. However, in the art of making high flux membranes, thin film composite (TFC) structure is regularly suggested by researchers. Using a TFC membrane made it possible to benefit from the good properties of selective layer for retention of solute and high porosity of support layer for increase of permeate flux.¹⁹ Anyhow, selective layer is main responsible for TFC membrane performance, and therefore, its chemical and morphological properties (depended to material selection) are important. Although hydrophilic surface assesses the improvement of membrane performance, hydrophobic polymers are still the most practical ones for preparation of UF membrane due to their superior chemical and thermal stability.²⁰ Accordingly, in the case of composite UF membranes, the use of Pebax copolymer as selective layer can be suitable due to its bicontinuous structure. In this case,

water molecules may transfer through poly(tetramethylene oxide) segments.²¹

The surface fouling is the main challenge in a HA removal via UF process and plays a crucial role on the membrane performance.²² Fouling leads to a decrease in membrane efficiency and the resultant flux even after backwashing.^{23,24} The common approach to reduce the membrane fouling is increment of membrane hydrophilicity.³ In this case, different hydrophilic materials are introduced as modifier by researchers. Inorganic additives, namely, TiO₂, Al₂O₃, SiO₂, ZrO₂, and ZnO, are a proper group of materials for this goal because of their ease of access and use.⁴ Among the mentioned additives, TiO₂ nanoparticles have been considered as an appropriate modifier because of their stability, commercial availability, ease of preparation, and their photocatalytic and super hydrophilic properties.²⁵

To modify polymeric membranes with nanoparticles like TiO₂, solution blending is the most common method. Anyhow, in some cases, this method leads to reduction of membrane permeability. Thus, other methods like coating technique are suggested by researchers.²⁶ For instance, Rahimpour et al²⁶ applied both coating and entrapping approaches for surface modification of polyethersulfone (PES) membranes by TiO₂ nanoparticles. They resulted that coating was more appropriate for surface modification and reduction of fouling when compared with entrapping method. Pourjafar et al²⁷ prepared a PVA (Poly Vinyl Alcohol)/PES composite membrane, which was modified by TiO₂ nanoparticles on the surfaces by coating method. The surface hydrophilicity and roughness of modified membranes were increased by coating of TiO₂ nanoparticles. Also, water permeability of the modified membranes was higher than that one for nascent membrane. Rajesh et al²⁴ investigated the effect of TiO₂ and combination ratio of polyamide imide (PAI) and polysulfone (PSf) polymers on the separation of HA from water. They resulted that incorporation of PAI and TiO₂ nanoparticles has a huge effect on improvement of morphology, hydrophilicity, pure water flux (PWF), rejection, and antifouling properties of PSf/PAI membranes. Anyhow, it should be notified that appropriate interaction between nanoparticles coating and selective layer increases the stability of nanoparticles on the surface of membrane.

According to author's findings, in the current study, UF-TFC membrane was prepared and modified to apply in the field of wastewater treatment. For this purpose, Pebax polymer was coated on the PES-PSf blend membrane as support layer. Indeed, PES-PSf blend membrane depicts smaller surface pores, higher porosity, and flux when compared with porous PSf membrane.^{28,29} Surface modification was performed using hydrophilic TiO₂ nanoparticles to improve hydrophilicity and antifouling properties of the prepared membrane. The prepared membranes were characterized and used for separation of HA from water.

2 | EXPERIMENTAL

2.1 | Materials

Polyethersulfone with M_w of 75 000 g mol⁻¹ and PSf with M_w of 60 000 g mol⁻¹ were obtained from BASF Company. Pebax 2533 was purchased from Arkema (France). Pebax 2533 is a member of

poly(ether-block-amide) copolymers, including 80 wt% soft poly(tetramethylene oxide) segments and 20 wt% hard polyamide 12 segments.^{30,31} TiO₂ nanoparticles (TiO₂, particle size of 21 nm, Degussa) were supplied by Evonik Company (Germany). *N*-Methyl-2-pyrrolidone and isobutanol from Merck were used as solvent. Distilled water as the nonsolvent was used in coagulation bath.

2.1.1 | Preparation of TFC membrane

The support membrane was fabricated via phase inversion induced by immersion precipitation technique. PSf and PES (1:1 w/w) were dissolved in *N*-methyl-2-pyrrolidone at 60°C for 15 hours under magnetic stirring to obtain 17 wt% polymeric solution. After degassing, the bubble-free solution was cast on a nonwoven polyester by a casting bar (Neurtek2281205) with a thickness of 250 μm. To solvent-nonsolvent exchange, the coated film was immediately immersed into a distilled water bath as nonsolvent at room temperature and kept for 24 hours to remove residual solvent. At the first step for preparation of selective layer, 10 wt% Pebax was dissolved in isobutanol at 90°C for 6 hours under reflux conditions to prepare coating solution. After degassing, the resultant solution was casted on the support membrane by a casting knife with a thickness of 3 μm and immediately placed in an oven at 80°C for 15 minutes.

2.1.2 | Membrane modification

For modification of TFC membrane, TiO₂ nanoparticles were dispersed in distilled water with concentrations of 0.01, 0.03, and 0.05 wt% followed by 1 hour sonication and being stirred vigorously for another 1 hour. Afterward, the prepared TFC membrane was immersed in TiO₂ colloidal suspensions for 1 hour. Finally, the coated membrane was washed by water and was dried at ambient temperature. The as-prepared membranes were coded according to the modifier loading (Table 1).

2.2 | Characterization tests

2.2.1 | FTIR analysis

Functional groups of as-prepared membranes were detected by Fourier transform infrared (FTIR) spectroscopy (Avatar 370 Nicolet, Spectrometer, USA). All FTIR spectra were presented in wavenumber range of 400 to 4000 cm⁻¹.

2.2.2 | SEM and FESEM analysis

The morphology of prepared membranes was investigated using scanning electron microscopy (SEM) (LEO 1450 VP, Zei, Germany) and field-emission SEM (FESEM) (SIGMA/VP, ZISS, Germany). For

TABLE 1 Introduction of prepared membranes

Membrane Sample	Code	TiO ₂ Concentration, wt%
Pebax/(PSf + PES)	TFC	0
0.01% TiO ₂ /Pebax/(PSf + PES)	TFN (0.01)	0.01
0.03% TiO ₂ /Pebax/(PSf + PES)	TFN (0.03)	0.03
0.05% TiO ₂ /Pebax/(PSf + PES)	TFN (0.05)	0.05

Abbreviations: PES, polyethersulfone; PSf, polysulfone; TFC, thin film composite; TFN, thin film nanocomposite.

making electrical conductivity, all samples were coated by gold sputtering. To have clean cuts for cross-sectional images, as-prepared membranes were broken in liquid nitrogen.

2.2.3 | Contact angle measurement

The water contact angles of the as-prepared membranes were measured by sessile drop technique by instrument (OCA15 plus, Dataphysics, Germany). The data of water contact angles are reported as the average of measurements obtained from at least 4 water droplets on each membrane surface.

2.2.4 | Membrane performance experiments

To measure the PWF, the membrane with effective area of 7.68 cm² was placed in contact with distilled water at a constant pressure, and the permeate volume and flux were measured every 10 minutes. This process was repeated with HA feed instead of water to measure the permeate flux. The concentration of HA in permeate was measured by a UV spectrophotometer (Optizen POP QX) in 254 nm wavelength.

According to the stable measured flux, pure water and permeate fluxes were calculated by the following equation.

$$J = \frac{V}{A \cdot \Delta t}, \quad (1)$$

where V denotes the permeate volume (L) and A and Δt are the membrane effective area (m²) and the permeate time (h), respectively.

The HA rejection factor was calculated as follows:

$$R(\%) = \left(1 - \frac{C_p}{C_f}\right) \times 100, \quad (2)$$

where R is the rejection factor and C_f and C_p denote the HA concentrations in feed and permeate, respectively.

2.2.5 | Membrane fouling resistance

One of the most important methods to investigate the membrane tendency for fouling is measuring the flux recovery ratio (FRR) after filtration of feed solution. To study the fouling resistance of as-prepared membranes, the PWF was measured for each membrane after 90 minutes at a specific pressure, in accordance to Equation 1. Then HA separation process was occurred, and permeate flux was calculated by passing 2 hours. Afterward, the membrane was washed with distilled water for 30 minutes, and then PWF measurement was repeated. Fouling-resistance properties of as-prepared membranes including FRR, reversible fouling ratio (R_r), and irreversible fouling ratio (R_{ir}) were calculated by following equations:

$$FRR = \frac{J_{w2}}{J_{w1}} \times 100, \quad (3)$$

$$R_r = \frac{J_{w2} - J_{HA}}{J_{w1}} \times 100, \quad (4)$$

$$R_{ir} = \frac{J_{w1} - J_{w2}}{J_{w1}} \times 100, \quad (5)$$

where J_{w1} is the initial PWF, J_{HA} is the permeate flux, and J_{w2} is the second PWF. All experiments were performed three times, and the average amount of the results was reported.

2.2.6 | HA adsorption experiment

To study the effect of adsorption characteristics of the membrane on its overall separation performance, adsorption tests were performed using a batch system. To do this, the as-prepared membranes were cut into circular pieces with 5 cm diameter and placed them into a HA solution of 20 mg/L in ambient temperature for 24 hours until reaching equilibrium. The HA concentration in the solution was analyzed before and after the adsorption process using a UV spectrophotometer at wavenumber of 254 nm. Finally, the HA adsorption capacity was calculated as follows:

$$\text{HA adsorption capacity}(\%) = \frac{C_0 - C}{A} \times 100, \quad (6)$$

where A is the membrane area and C_0 and C are the HA solution concentration before and after adsorption process, respectively.

3 | RESULTS AND DISCUSSION

3.1 | Membrane characterization

3.1.1 | FTIR analysis

Figure 1 illustrates the FTIR spectrum of TiO₂ nanoparticles and TFC and Thin Film Nanocomposite (TFN) membranes. For TiO₂, in Figure 1A, the bands which observed in the range of 450 to 800 cm⁻¹ are related to the stretching vibrations of Ti—O—Ti and Ti—O groups on the surface of TiO₂ nanoparticles.^{32,33} The bands at 1627 and 3398 cm⁻¹ correspond to the stretching vibration of —OH groups on nanoparticles surface.^{34,35} The FTIR analysis of Pebax film is given in Figure 1B. The band at 1112 and 1740 cm⁻¹ is attributed to the C—O—C and —C=O stretching vibrations, respectively. Also, another 2 bands at 1640 and 3308 cm⁻¹ are assigned to the presence of H—N—C=O and N—H groups, in the hard Polyamide (PA) segment, respectively.^{30,36} In FTIR spectra of Pebax (Figure 1B), it seems that PA block of Pebax is significantly self-associated via hydrogen bonding.³⁶ The FTIR spectrum of PSf-PES support membrane is illustrated in Figure 1C. The observed bands at 1110, 1240, 1150, and 1323 cm⁻¹ are corresponded to vibrations of C—O, C—O—C, and symmetric and asymmetric O=S=O groups of PSf and PES, respectively. Also,

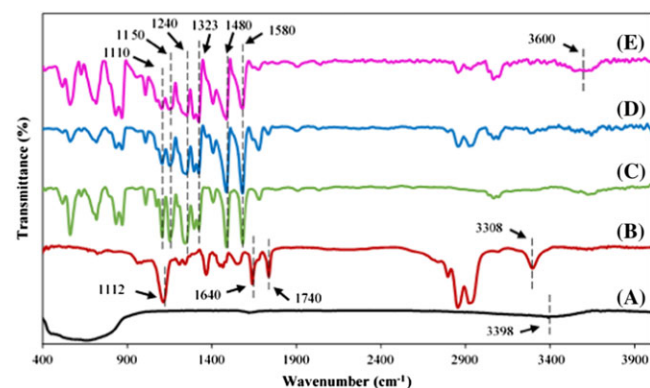


FIGURE 1 Fourier transform infrared spectra of, A, TiO₂ nanoparticles, B, Pebax membrane, C, support membrane (polyethersulfone + polysulfone), D, thin film composite membrane, and, E, thin film nanocomposite (0.03) membrane [Colour figure can be viewed at wileyonlinelibrary.com]

the bands around 1480 to 1580 cm^{-1} are related to aromatic ring stretching vibrations of asymmetric C=C.^{28,33-35} In Figure 1D, the results of FTIR analysis for TFC membrane are shown. It is clear that all of the peaks in the FTIR spectra of Pebax film and support membrane are observed in FTIR analysis of TFC membrane.

A comparison between the FTIR spectra of TFC membrane and TFN (0.03) membrane (Figure 1E) reveals that in the spectrum of coated membrane (Figure 1E), the bands around 500 to 800 cm^{-1} are attributed to the presence of TiO_2 nanoparticles on the membrane surface. In addition, the broad peak around 3500 to 3700 cm^{-1} is augmented the presence of significant amount of OH groups of TiO_2 nanoparticles on membrane surface (Figure 1E). It is also observed that a considerable amount of amide groups contributing to the spectrum of Pebax disappear after modification of membrane by TiO_2 nanoparticles coating. This suggests that the interchain hydrogen bonding between the amide groups of Pebax chains at surface of membrane is partially broken by the presence of TiO_2 nanoparticles. This behavior was reported in previous studies, which focus on the effect of nanoparticles on Pebax membrane structure via solution blending method.³⁷ These results can propose the interaction between TiO_2 nanoparticles and Pebax polymer chains.

3.1.2 | Contact angle

Contact angle analysis was conducted to investigate the effect of TiO_2 nanoparticles on hydrophilicity of the membranes. The surface contact angle of prepared TFC and TFN membranes are presented in Table 2. The results clearly show that the contact angle decreases by increase of TiO_2 nanoparticles concentration from 73.76° for TFC to 58.36° for TFN (0.05). The contact angle is inversely related to the hydrophilicity. Therefore, adding TiO_2 nanoparticles improves the hydrophilicity of the membranes.³⁸ Hydroxyl groups of TiO_2 nanoparticles have caused the possibility of interacting with amide groups of Pebax by OH species. On the other side, hydrophilicity of membrane surface has been improved by hydroxyl groups due to their polarity that facilitates the interaction with water molecules.³⁹ This conclusion is in line with the results of Luo et al⁴⁰ who reported that by increase of TiO_2 nanoparticles, the hydrophilicity of modified membrane is increased.

3.1.3 | Morphological studies

Figure 2 represents surface morphologies of TFC and modified TFC membranes using FESEM technique. A comparison between the surface FESEM images of TFC and TFN membranes indicates that the selective Pebax layer of TFC membrane has no nanoparticles or any deflection on its surface. On the other side, little white spots were observed on the surface of TFN membrane selective layer. This spots

confirm that deposition of TiO_2 nanoparticles is well done.⁴¹ As clearly seen in this figure, at high concentration of TiO_2 , aggregation of nanoparticles has induced on the top surface of modified TFC membrane.²⁶

Figure 3A depicts the FESEM image of the selective TiO_2 -coated Pebax layer. This figure confirms that the selective layer was properly coated on the support membrane. Also, it has clearly been observed that TiO_2 nanoparticles are successfully coated and well dispersed on the membrane surface.³⁹ Figure 3B illustrates the surface morphology of TFN (0.03) membrane after PWF experiments. As can be seen, even after permeation and washing, TiO_2 nanoparticles are not removed from surface of selective layer. This can be attributed to the strong bonding between TiO_2 nanoparticles and polymeric structure of the membrane²⁶ and was previously confirmed by FTIR results. Figure 3C represents the cross-sectional image of the TFN (0.03) membrane. While TiO_2 nanoparticles are deposited only on the surface of membrane, cross-sectional structure of all TFN membranes is similar to TFC membranes.⁴¹ Additionally, as depicted in Figure 3C, the membrane exhibits an asymmetric structure, consisted of a selective Pebax layer with an approximate thickness of 1 to 2 μm , which has successfully coated on finger-like support layer.

3.2 | Membrane performance

3.2.1 | Pure water flux

The PWF of prepared membranes with different TiO_2 nanoparticles concentration at the pressures of 3 and 5 bar is depicted in Figure 4A. Increase of hydrophilicity and clogging of surface tiny pores, which are the results of addition of TiO_2 nanoparticles, have 2 antithetical effects on the flux. By addition of TiO_2 , the PWF first dropped, which is followed by a raise and another drop. As seen in Figure 4A, the PWF of TFN (0.01) membrane is lower than TFC membrane, which is due to pore clogging by TiO_2 nanoparticles that overcomes the effect of hydrophilicity increase. Bae and Tak³⁸ have reported similar observations for PSF membranes in which the results showed that by addition of TiO_2 nanoparticles to the membrane, the flux decreased. They mentioned that this behavior might be due to the plugging of some pores on membrane surfaces.

As the concentration of TiO_2 nanoparticles increase up to 0.03%, hydrophilicity is also increased, which results in the adsorption of water molecules, facilitates the penetration through the membrane, and leads to the maximum value of PWF. At high TiO_2 loading (TFN (0.05)), the aggregation phenomenon of nanoparticles leads to a lower contribution of hydrophilicity to the flux. In a similar study, Madaeni and Ghaemi³⁹ reported that at high TiO_2 concentration, the PWF was reduced due to agglomeration of nanoparticles.

In addition, a comparison between the PWF results at 2 different operating pressures (3 and 5 bars) for all the as-prepared membranes shows a slight enhancement by increase of pressure. Generally, the PWF is usually in direct relation with applied hydrostatic pressure. In this condition, by increase of pressure, passing rate of water molecules through the membrane increases. The observed trend is related to the driving force enhancement and its beat to membrane resistance. Ahmad et al⁴² observed a similar effect of operating pressure on flux in UF membrane where flux increased with elevating the operating pressure from 16.2 to 18.2 psi.

TABLE 2 Contact angle of prepared membranes

Membrane	Contact Angle, °
TFC	73.76 ± 0.13
TFN (0.01)	66.36 ± 0.23
TFN (0.03)	62.5 ± 0.24
TFN (0.05)	58.36 ± 0.17

Abbreviations: TFC, thin film composite; TFN, thin film nanocomposite.

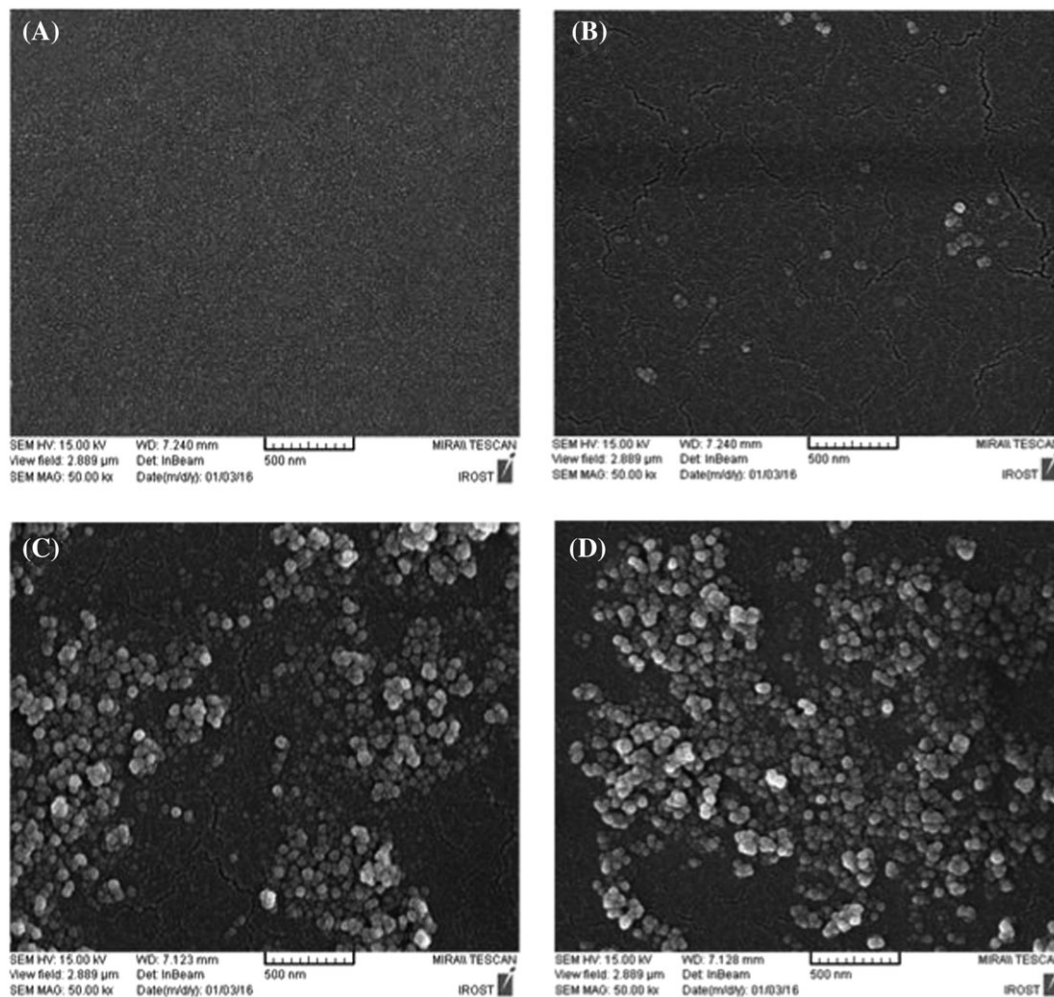


FIGURE 2 Field emission scanning electron microscopy surface images of, A, thin film composite, B, thin film nanocomposite (TFN) (0.01), C, TFN (0.03), and, D, TFN (0.05)

3.2.2 | HA rejection ratio and permeate flux

Figure 4B illustrates permeate flux values versus TiO_2 concentration at different pressures. As can be seen, the effect of applied pressure on the permeate flux is similar to its effect on PWF.²⁶ The comparison between PWF and permeate flux for each prepared membrane at a specific pressure shows that the permeate flux is lower than the PWF. In UF membranes, PWF is proportional to the applied pressure and has an inverse relation to hydrodynamic resistance of the membrane. The adsorption of HA on the surface or pore plugging may cause an additional resistance against the pass of feed flow.⁴³

The performance of prepared membranes in terms of HA rejection at different pressures is illustrated in Figure 4C. The results show that the rejection is enhanced for modified membranes in comparison with TFC membranes. As discussed above, the presence of TiO_2 nanoparticles on the surface results in enhancement of membrane hydrophilicity, which causes more interactions between water molecules and nanoparticles and formation of thin water layer.⁴⁴

As seen in Figure 4C, HA rejection of TFN (0.01) is the maximum among the other membranes. It can be said that in TFN (0.01) membrane, TiO_2 nanoparticles plug surface pores, which cause prevention of HA passing and lead to improvement of rejection ratio. However, by increasing extra amount of nanoparticles, they agglomerate and heterogeneously

distribute on the surface of membranes. Accordingly, HA molecules can reach membrane surface and transport through the pores, which lead to reduction of HA rejection.⁴⁵ In another study, Song et al⁴⁶ observed that pepsin rejection of Polyvinylidene fluoride (PVDF)/Polyethylene glycol (PEG) membrane, which was modified by TiO_2 nanoparticles, decreased at a higher TiO_2 loading. They concluded that by increase of TiO_2 concentration, aggregated particles were formed on the membrane surface.

The comparison between the experimental results of all membranes at different operating pressures (Figure 4C) shows a smooth decrease of HA rejection by increase of pressure. The increase in feed pressure will increase the driving force, which overcomes the membrane resistance and leads to more HA molecules passing through the membrane. In addition, increasing the pressure causes accumulation of HA molecules on the membrane surface, which can decrease the hydrophilicity. Therefore, the rejection is decreased with pressure at constant feed concentration.⁴² In a research of oil removal from water using membrane separation technique, Madaeni et al⁴⁷ resulted that accumulation of oil droplets on the membrane surface caused decrease of hydrophilicity property on the surface that led to more pass of oil through the membrane and thus reduction of rejection.

The effect of feed concentration on the permeate flux and HA rejection of TFN (0.03) sample at a constant pressure of 3 bars is

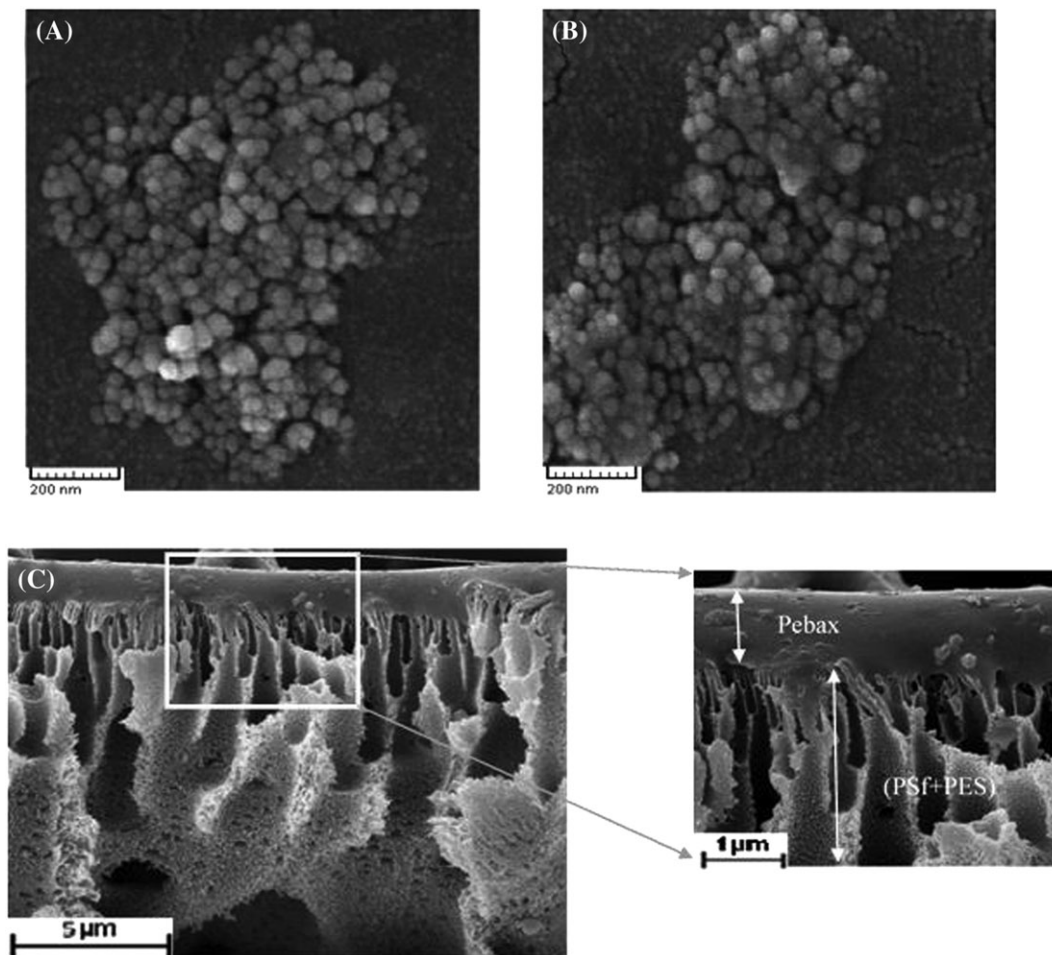


FIGURE 3 A, Field emission scanning electron microscopy image of top surface of thin film nanocomposite (TFN) (0.03), B, top surface of TFN (0.03) after pure water flux test, and, C, scanning electron microscopy image of cross section of TFN (0.03)

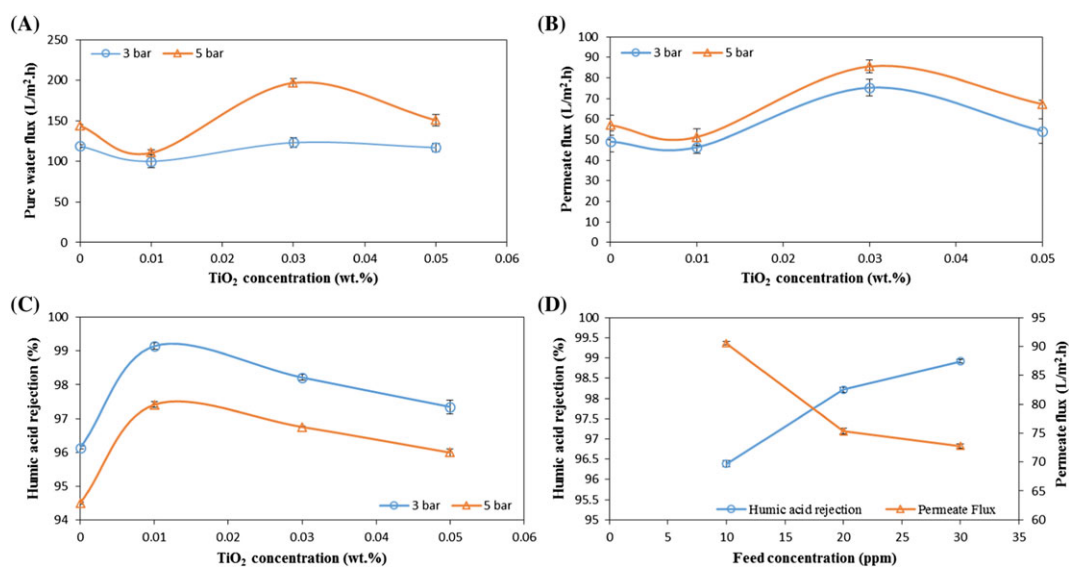


FIGURE 4 A, Pure water flux, B, permeate flux, C, humic acid rejection, D, humic acid rejection and permeate flux in different feed concentrations of TFN (0.03) at $P = 3$ bar, of membranes [Colour figure can be viewed at wileyonlinelibrary.com]

presented in Figure 4D. A decrease in permeate flux is observed with an increase of feed concentration from 10 to 30 ppm. It can be concluded that the increase of feed concentration results in more

concentration polarization and as a consequence increase of fouling possibility in UF membranes.⁴⁸ The deposited HA on the surface of membrane plays the role of an additional resistance to feed flow pass

and decreases the permeate flux. On the other hand, HA rejection increases with increase of feed concentration. The mentioned additional resistance causes lower permeation of HA through the membrane, and therefore, HA rejection enhances.^{42,43}

3.2.3 | HA adsorption

Figure 5 shows HA adsorption capacity of the prepared membranes with different concentrations of TiO₂. As experimental results illustrate, with increasing TiO₂ loading, the amount of adsorbed HA is increased from 2.58 mg/cm² for TFC to 6.51 mg/cm² for TFN (0.03) sample. The adsorption of HA occurs mainly because of electrostatic interaction between TiO₂ and carboxylate groups of HA and hydrogen bonding interactions between these carboxylates and OH groups of TiO₂.^{49,50} The increase of adsorption would be because of the increase

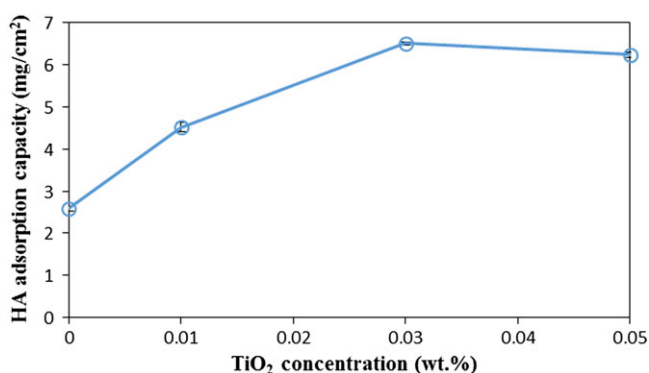


FIGURE 5 Effect of TiO₂ concentration on humic acid (HA) adsorption of membranes [Colour figure can be viewed at wileyonlinelibrary.com]

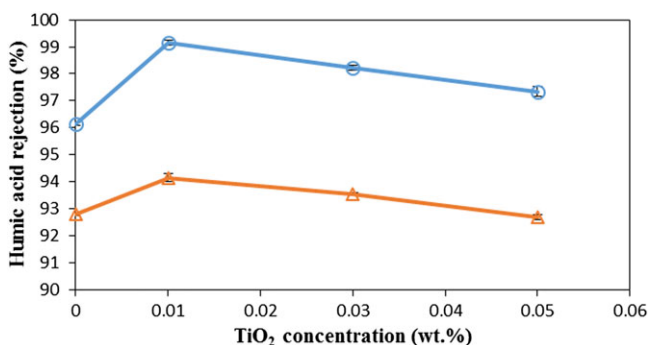


FIGURE 6 Humic acid rejection of membranes (○ before adsorption and △ after adsorption) [Colour figure can be viewed at wileyonlinelibrary.com]

in the number of active accessible adsorption sites. At high TiO₂ loading (0.05 wt%), as mentioned in previous sections, the agglomeration phenomenon of nanoparticles is occurred, which causes a decrease in access to the active adsorption sites. Therefore, adsorption capacity of the membrane with 0.05 wt% TiO₂ is lower than that of TFN (0.03) sample.

Regarding to the high value of HA rejection for all the prepared membranes, the role of membranes in 2 aspects of adsorption and membrane filtration is investigated. Therefore, HA rejection is compared before and after adsorption process for the membranes, which is illustrated in Figure 6. For this purpose, HA rejection ratio of a membrane after adsorption test is compared with the ratio of a similar membrane without any adsorption process. The results show that the HA rejection for modified TFC membranes decreases from 99.14% before adsorption process to 94.15% after adsorption process. In addition, this decrease can be seen for TFC membrane, which is from 96.14% before adsorption process to 92.78% after adsorption process. This trend shows that adsorption process also occurred in the membrane without any TiO₂ nanoparticles. This comparison between the value of HA rejection before and after adsorption process confirms that the effect of adsorption process on the removal of HA from water is negligible, and the main factor involved in this separation is membrane filtration.

3.2.4 | Membrane fouling analysis

The calculated values of FRR, reversible fouling ratio (R_r), and irreversible fouling ratio (R_{ir}) are presented in Table 3. The results indicate that FRR value of membrane increases from 50.69% for TFC membrane to 72.74% for TFN (0.03), while R_{ir} and R_r values were decreased and increased, respectively. By looking at the results, it is observed that FRR value and antifouling properties are improved in the modified membranes. This improvement is due to increase in hydrophilicity and reduction of interactions between the contaminant and membrane surface.²⁶ The increase in hydrophilicity facilitates the presence of a thin layer of water on membrane surface, which suggests that the HA fouling in modified TFC membranes is reversible and can easily be eliminated by washing.⁴⁴ However, FRR value of TFN membranes decreases at 0.05 wt% TiO₂ concentration. As discussed in previous sections, the increase in TiO₂ concentration to 0.05 wt% causes agglomeration. This result in lower rejection of HA in some parts of the membrane and as a consequence increase of R_{ir} and decrease of FRR. Accordingly, the amount of TiO₂ for modification of the membrane surface should be optimized.⁴⁶ In a related study, Luo et al⁴⁰ observed that the antifouling performance of the PES UF membrane

TABLE 3 FRR, R_r , and R_{ir} values of prepared membranes

Membrane	FRR		R_{ir}		R_r	
	3 bar	5 bar	3 bar	5 bar	3 bar	5 bar
TFC	50.69 ± 0.06	45.31 ± 0.04	49.31 ± 0.06	54.69 ± 0.03	8.33 ± 0.17	5.68 ± 0.06
TFN (0.01)	55.57 ± 0.09	52.41 ± 0.04	44.43 ± 0.12	47.59 ± 0.05	9.32 ± 0.09	6.06 ± 0.18
TFN (0.03)	72.74 ± 0.06	54.09 ± 0.02	27.25 ± 0.17	45.9 ± 0.03	11.63 ± 0.26	10.62 ± 0.09
TFN (0.05)	57.67 ± 0.01	52.63 ± 0.09	42.32 ± 0.02	47.36 ± 0.09	11.45 ± 0.15	8.38 ± 0.03

Abbreviations: FRR, flux recovery ratio; TFC, thin film composite; TFN, thin film nanocomposite.

TABLE 4 Comparison of HA removal reported of literatures with prepared membranes in this study

Membrane	Membrane Process	Filler	Pressure, bar	Permeate Flux, L/m ² ·h	HA Rejection, %	FRR, %	Ref.
PEI	UF	PEG	3	188	56	42.68	Hwang et al ²³
PES	UF	GA	3	24	87	88	Mehrpour et al ⁵¹
PES	UF	DBA	3	26	81	73	Mehrpour et al ⁵¹
PAN	UF	CS + Fe ₃ O ₄	5.5	25.5	96.5	...	Rekha Panda et al ⁴⁸
RC	UF	Negatively charge (sulfonic acid group)	1	...	91	67	Shao et al ⁵²
RC	UF	Negatively charge (carboxylic acid group)	1	...	96	56	Shao et al ⁵²
Cellulose acetate	UF	OMMT	3	160	95.047	...	Sabet Dehkordi et al ¹⁸
PVDF	UF	PEG	1	...	83	58	Song et al ⁴⁶
PVDF	UF	TiO ₂	1	...	88	63	Song et al ⁴⁶
TFN (0.03)	UF	TiO₂	3	75.32	98.22	72.74	This study
TFN (0.01)	UF	TiO₂	3	46.32	99.14	55.57	This study

Abbreviations: CS, chitosan; DBA, diaminobenzoic acid; FRR, flux recovery ratio; GA, gallic acid; OMMT, Organically modified montmorillonite; PAN, Polyacrylonitrile; PES, polyethersulfone; PEI, Polyetherimide; RC, regenerated cellulose; TFN, thin film nanocomposite; UF, ultrafiltration.

was improved by coating TiO₂ nanoparticles on the membrane surface. They offered coating of TiO₂ nanoparticles as a strong potential type of antifouling technique.

As seen in Table 3, increasing the pressure leads to the increase of R_{ir} and decrease of R_r . The increase of pressure in UF membranes, as the driving force, causes concentration polarization in the feed side, the increase of fouling phenomena, and formation of a cake layer on the membrane. These factors are the main reasons for increase of R_{ir} and decrease of R_r with pressure.⁴³

Table 4 compares the results of the present study with some published studies in the literatures regarding permeate flux, rejection, and FRR for HA removal from water, although the conditions under which the experiments were performed are not exactly the same. According to Table 4, the HA rejection value for the prepared membranes of this study is comparable with the other membranes used in the other studies; however, the simultaneous improvement of HA rejection, permeate flux, and FRR makes a superiority for this study in comparison with the others.

4 | CONCLUSIONS

In this study, a composite membrane consisted of a selective Pebax layer on a porous PES/PSf blend support was prepared for removal of HA from water. To modify the prepared membrane, its surface was coated with hydrophilic TiO₂ nanoparticles of different concentrations (0.01, 0.03, and 0.05 wt%). The SEM and FESEM images showed that the selective Pebax layer was successfully coated on the porous support, and nanoparticles were properly distributed on the surface of membrane. Also, at a higher TiO₂ loading, an agglomeration phenomenon of nanoparticles occurred. The results of FTIR and contact angle analysis confirmed that the presence of TiO₂ nanoparticles enhanced membrane hydrophilicity. Furthermore, the performance of prepared membranes was investigated in terms of the PWF, permeate flux, HA rejection, solute adsorption, and antifouling properties under different operating pressures and feed concentrations. The results

showed that the membrane hydrophilicity and tiny pores blocked by TiO₂ nanoparticles have 2 different effects on the flux, and the best PWF value was observed in TFN (0.03) membrane. On the other hand, the addition of TiO₂ nanoparticles improved HA rejection and the antifouling properties of the prepared membranes. The main mechanism involved in the separation procedure was membrane filtration. The prepared nanocomposite membranes were compared with the membranes used in other studies. Humic acid rejection of TFN (0.01) membrane in present study proposes the best rejection value compared to that one of membranes in the other studies.

ORCID

Naeema Cheshomi  <http://orcid.org/0000-0002-1280-1142>

REFERENCES

- Aiken GR, McKnight DM, Wershaw RL, MacCarthy P. Humic substances in soils, sediments and water: geochemistry, isolation and characteristics. *Geol J.* 1985;21:213-214.
- Gutman IS, Semiat R. Humic substances fouling in ultrafiltration processes. *Desalination.* 2010;261:218-231.
- Hamid NAA, Ismail AF, Matsuura T, et al. Morphological and separation performance study of polysulfone/titanium dioxide (PSF/TiO₂) ultrafiltration membranes for humic acid removal. *Desalination.* 2011;273:85-92.
- Yuan W, Zydney AL. Humic acid fouling during microfiltration. *J Membr Sci.* 1999;157:1-12.
- Xue G, Liu H, Chen Q, Hills C, Tyrer M, Innocent F. Synergy between surface adsorption and photocatalysis during degradation of humic acid on TiO₂/activated carbon composites. *J Hazard Mater.* 2011;186:722-765.
- Feng J, Zhu BW, Lim TT. Reduction of chlorinated methanes with nano-scale Fe particles: effects of amphiphiles on the dechlorination reaction and two-parameter regression for kinetic prediction. *Chemosphere.* 2008;73:1817-1823.
- Zulfikar MA, Afrita S, Wahyuningrum D, Ledyastuti M. Preparation of Fe₃O₄-chitosan hybrid nano-particles used for humic acid adsorption. *Environ. Nanotechnology, Monitoring Management.* 2016;6:64-75.

8. Oskoei V, Dehghani MH, Nazmara S, et al. Removal of humic acid from aqueous solution using UV/ZnO nano-photocatalysis and adsorption. *J Mol Liq.* 2016;213:374-380.
9. Trellu C, Péchaud Y, Oturan N, et al. Comparative study on the removal of humic acids from drinking water by anodic oxidation and electro-Fenton processes: mineralization efficiency and modelling. *Appl Catal B.* 1943;2016:2-41.
10. Čehovin M, Medic A, Scheideler J, et al. Hydrodynamic cavitation in combination with the ozone, hydrogen peroxide and the UV-based advanced oxidation processes for the removal of natural organic matter from drinking water. *Ultrason Sonochem.* 2017;37:394-404.
11. Wang W, Feng P, Yang Q, Wang W, Wang X. Effects of sodium, magnesium, and calcium salts on the coagulation performance of cucurbit [8]uril for humic acid removal from synthetic seawater. *Desalination.* 2016;386:77-83.
12. Xu Y, Chen T, Cui F, Shi W. Effect of reused alum-humic-flocs on coagulation performance and floc characteristics formed by aluminum salt coagulants in humic-acid water. *Chem Eng J.* 2016;287:225-232.
13. Sathish Kumar R, Arthanareeswaran G, Paul D, Hyang KJ. Effective removal of humic acid using xanthan incorporated polyethersulfone membranes. *Ecotox Environ Safe.* 2015;121:223-228.
14. Shankar V, Heo J, Al-Hamadani YAJ, Park CM, Chu KH, Yoon Y. Evaluation of bichar-ultrafiltration membrane processes for humic acid removal under various hydrodynamic, pH, ionic strength, and pressure conditions. *J Environ Manage.* 2017;197:610-618.
15. Kanagraj P, Nagendran A, Rana D, Matsuura T. Separation of macromolecular proteins and removal of humic acid by cellulose acetate modified UF membranes. *Int J Biol Macromol.* 2016;89:81-88.
16. Song JJ, Huang Y, Nam SW, et al. Ultrathin graphene oxide membranes for the removal of humic acid. *Sep Purif Technol.* 2015;144:162-167.
17. Wang J, Lang WZ, Xu HP, Zhang X, Guo YJ. Improved poly(vinyl butyral) hollow fiber membranes by embedding multi-walled carbon nanotube for the ultrafiltrations of bovine serum albumin and humic acid. *Chem Eng J.* 2015;260:90-98.
18. Sabet Dehkordi F, Pakizeh M, Namvar-Mahboub M. Properties and ultrafiltration efficiency of cellulose acetate/organically modified Mt (CA/OMMT) nanocomposite membrane for humic acid removal. *Appl Clay Sci.* 2015;105 - 106:178-185.
19. Namvar-Mahboub M, Pakizeh M. Development of a novel thin film composite membrane by interfacial polymerization on polyetherimide/modified SiO₂ support for organic solvent nanofiltration. *Sep Purif Technol.* 2013;119:35-45.
20. Nunes SP, Sforqa ML, Peinemann KV. Dense hydrophilic composite membranes for ultrafiltration. *J Membr Sci.* 1995;106:49-56.
21. Shahkarampour N, Tran TN, Ramanan S, Lin H. Membranes with surface-enhanced antifouling properties for water purification. *Membranes.* 2017;7:13-30.
22. Mazloomi S, Nabizadeh R, Nasserli S, Naddafi K, Nazmara S, Mahvi AH. Efficiency of domestic reverse osmosis in removal of trihalomethanes from drinking water. *Iran J Environ Health Sci Eng.* 2009;6:16-30.
23. Hwang LL, Tseng HH, Chen JC. Fabrication of polyphenylsulfone/polyetherimide blend membranes for ultrafiltration applications: the effects of blending ratio on membrane properties and humic acid removal performance. *J Membr Sci.* 2011;384:72-81.
24. Rajesh S, Senthilkumar S, Jayalakshmi A, Nirmala MT, Ismail AF, Mohan D. Preparation and performance evaluation of poly (amide-imide) and TiO₂ nanoparticles impregnated polysulfone nanofiltration membranes in the removal of humic substances. *Colloid Surface A.* 2013;418:92-104.
25. Sotro A, Boromand A, Zhang R, et al. Effect of nanoparticle aggregation at low concentration of TiO₂ on the hydrophilicity, morphology, and fouling resistance of PES-TiO₂ membranes. *J Colloid Interface Sci.* 2011;363:540-550.
26. Rahimpour A, Madaeni SS, Taheri AH, Mansourpanah Y. Coupling TiO₂ nanoparticles with UV irradiation for modification of polyethersulfone ultrafiltration membranes. *J Membr Sci.* 2008;313:158-169.
27. Pourjafar S, Rahimpour A, Jahanshahi M. Synthesis and characterization of PVA/PES thin film composite nanofiltration membrane modified with TiO₂ nanoparticles for better performance and surface properties. *J Ind Eng Chem.* 2012;18:1398-1405.
28. Pagidi A, Saranya R, Arthanareeswaran G, Ismail AF, Matsuura T. Enhanced oil-water separation using polysulfone membranes modified with polymeric additives. *Desalination.* 2014;344:280-288.
29. Sun Y, Xue L, Zhang Y, Zhao X, Huang Y, Du X. High flux polyamide thin film composite forward osmosis membranes prepared from porous substrates made of polysulfone and polyethersulfone blends. *Desalination.* 2014;336:72-79.
30. Le NL, Wang Y, Chung TS. Pebax/POSS mixed matrix membranes for ethanol recovery from aqueous solution via pervaporation. *J Membr Sci.* 2011;379:174-183.
31. Bernardo P, Jansen JC, Bazzarelli F, et al. Gas transport properties of Pebax/room temperature ionic liquid gel membranes. *Sep Purif Technol.* 2012;97:73-82.
32. Sairam M, BPatil M, S Veeapur R, APatil S, MAminabhavi T. Novel dense poly(vinyl alcohol)-TiO₂ mixed matrix membranes for pervaporation separation of water-isopropanol mixtures at 30°C. *J Membr Sci.* 2006;281:95-102.
33. Emadzadeh D, Lau WJ, Matsuura T, Rsisakht M, Ismail AF. A novel thin film composite forward osmosis membrane prepared from PSF-TiO₂ nanocomposite substrate for water desalination. *Chem Eng J.* 2014;237:70-80.
34. Zhang G, Lu S, Zhang L, Meng Q, Shen C, Zhang J. Novel polysulfone hybrid ultrafiltration membrane prepared with TiO₂-g-HEMA and its antifouling characteristics. *J Membr Sci.* 2013;436:163-173.
35. Razmjou A, Mansouri J, Chen V. The effects of mechanical and chemical modification of TiO₂ nanoparticles on the surface chemistry, structure and fouling performance of PES ultrafiltration membranes. *J Membr Sci.* 2011;378:73-84.
36. Kim JH, Lee YM. Gas permeation properties of poly(amide-6-b-ethylene oxide)-silica hybrid membranes. *J Membr Sci.* 2001;193:209-225.
37. Azizi N, Mohammadi T, Mbehbahani R. Comparison of permeability performance of Pebax-1074/TiO₂, Pebax-1074/SiO₂, and Pebax-1074/Al₂O₃ nanocomposite membranes for CO₂/CH₄ separation. *Chem Eng Res Des.* 2017;117:177-189.
38. Bae TH, Tak TM. Effect of TiO₂ nanoparticles on fouling mitigation of ultrafiltration membranes for activated sludge filtration. *J Membr Sci.* 2005;249:1-8.
39. Madaeni SS, Ghaemi N. Characterization of self-cleaning RO membranes coated with TiO₂ particles under UV irradiation. *J Membr Sci.* 2007;303:221-233.
40. Luo ML, Zhao JQ, Tang W, Pu CS. Hydrophilic modification of poly(ether sulfone) ultrafiltration membrane surface by self-assembly of TiO₂ nanoparticles. *Appl Surf Sci.* 2005;249:76-84.
41. Moghimifar V, Raisi A, Aroujalian A. Surface modification of polyethersulfone ultrafiltration membranes by corona plasma-assisted coating TiO₂ nanoparticles. *J Membr Sci.* 2014;461:69-80.
42. Ahmad AL, Puasa SW, Abiding S. Cross-flow ultrafiltration for removing direct-15 dye from wastewater of textile industry. *ASEAN J Sci Technol Develop.* 2006;23(3):207-216.
43. Mulder M. *Basic Principles of Membrane Technology.* Boston: Kluwer Academic Publishers; 1996.
44. Li JB, Zhu JW, Zheng MS. Morphologies and properties of poly(phthalazinone ether sulfone ketone) matrix ultrafiltration membranes with entrapped TiO₂ nanoparticles. *J Appl Polym Sci.* 2006;103:2623-3629.
45. Yang Y, Zhang H, Wang P, Zheng Q, Li J. The influence of nano-sized TiO₂ fillers on the morphologies and properties of PSf UF membrane. *J Membr Sci.* 2007;288:231-238.

46. Song H, Shao J, He Y, Liu B, Zhong X. Natural organic matter removal and flux decline with PEG-TiO₂-doped PVDF membranes by integration of ultrafiltration with photocatalysis. *J Membr Sci*. 2012;405–406:48–56.
47. Madaeni S, Gheshlaghi A, Rekabdar F. Membrane treatment of oily wastewater from refinery processes. *Asia-Pacific J Chem Eng*. 2013;8:45–53.
48. Rekha Panda S, Mukherjee M, De S. Preparation, characterization and humic acid removal capacity of chitosan coated iron-oxide-polycrylonitrile mixed matrix. *J Water Proc Eng*. 2015;6:93–104.
49. Sun DD, Lee PF. TiO₂ microsphere for the removal of humic acid from water: complex surface adsorption mechanisms. *Sep Purif Technol*. 2012;91:30–37.
50. Liu S, Lim M, Amal R. TiO₂-coated natural zeolite: rapid humic acid adsorption and effective photocatalytic regeneration. *Chem Eng Sci*. 2014;105:46–52.
51. Mehrparvar A, Rahimpour A, Jahanshahi M. Modified ultrafiltration membranes for humic acid removal. *J Taiwan Inst Chem Eng*. 2013;45(1):275–282.
52. Shao J, Zhao L, Chen X, He Y. Humic acid rejection and flux decline with negatively charged membranes of different spacer arm lengths and charge groups. *J Membr Sci*. 2013;435:38–45.

How to cite this article: Cheshomi N, Pakizeh M, Namvar-Mahboub M. Preparation and characterization of TiO₂/Pebax/(PSf-PES) thin film nanocomposite membrane for humic acid removal from water. *Polym Adv Technol*. 2018;29:1303–1312. <https://doi.org/10.1002/pat.4242>